The hepatitis C virus NS2 protein is an inhibitor of CIDE-B-induced apoptosis

L. Erdtmann, Nicolas Franck, H. Lerat, J. Le Seyec, D. Gilot, I. Cannie, P. Gripon, U. Hibner, C. Guguen-Guillouzo

THE JOURNAL OF BIOLOGICAL CHEMISTRY
Vol. 278, No. 20, Issue of May 16, pp. 18256–18264, 2003
Printed in U.S.A.

The Hepatitis C Virus NS2 Protein Is an Inhibitor of CIDE-B-induced Apoptosis*

Received for publication, September 23, 2002, and in revised form, January 27, 2003
Published, JBC Papers in Press, February 20, 2003, DOI 10.1074/jbc.M209732200

Lars Erdtmann‡§, Nathalie Franck‡¶, Hervé Lerat‖, Jacques Le Seyec‡, David Gilot‡, Isabelle Cannie‡, Philippe Gripon‡, Urszula Hibner‖, and Christiane Guguen-Guillouzo‡

From ‡INSERM U522, Hôpital de Pontchaillou, 35033 Rennes Cedex, France and ‖CNRS UMR 5535, Institut de Génétique Moléculaire, 34293 Montpellier Cedex 5, France

Chronic hepatitis C virus (HCV) infection frequently leads to liver cancer. To determine the viral factor(s) potentially involved in viral persistence, we focused our work on NS2, a viral protein of unknown function. To assign a role for NS2, we searched for cellular proteins that interact with NS2. Performing a two-hybrid screen on a human liver cDNA library, we found that NS2 interacted with the liver-specific pro-apoptotic CIDE-B protein. Binding specificity of NS2 for CIDE-B was confirmed by cell-free assays associated with colocalization studies and coprecipitation experiments on human endogenous CIDE-B. CIDE-B, a member of the novel CIDE family of apoptosis-inducing factors, has been reported to show strong cell death-inducing activity in its C-terminal domain. We show that this CIDE-B killing domain is involved in the NS2 interaction. NS2 binding was sufficient to inhibit CIDE-B-induced apoptosis because an NS2 deletion mutant unable to interact with CIDE-B *in vitro* lost its capacity to interfere with CIDE-B cell death activity. Although it has been reported that CIDE-B-induced apoptosis is characterized by mitochondrial localization, the precise apoptotic mechanism remained unknown. Here, we show that CIDE-B induced cell death in a caspase-dependent manner through cytochrome *c* release from mitochondria. Furthermore, we found that NS2 counteracted the cytochrome *c* release induced by CIDE-B. *In vivo*, the CIDE-B protein level was extremely low in adenovirus-infected transgenic mice expressing the HCV polyprotein compared with that in wild-type mice. We suggest that NS2 interferes with the CIDE-B-induced death pathway and participates in HCV strategies to subvert host cell defense.

Of the different antiviral defense systems developed by the cell, programmed cell death, or apoptosis, significantly contributes to the prevention of viral replication, dissemination, and persistence (1, 2). To survive, viruses elaborate multiple protective strategies that could interfere at different levels of the process leading to cell death. The complex molecular program of apoptosis may be initiated by intrinsic or extrinsic signals. Recently, the double-stranded RNA-dependent protein kinase PKR has been shown to play a critical role as an intracellular stimulus in mediating double-stranded RNA-induced apoptosis via the activation of the Fas-associated death domain signaling cascade (3–5). This Fas-associated death domain-mediated death signaling pathway is also activated by extrinsic signals such as Fas ligand and tumor necrosis factor-α (6–8). The binding of Fas ligand to its Fas/APO-1/CD95 cell-surface death receptor triggers the activation of caspase-8, which thereupon can directly cleave procaspase-3 in its activated form (9). Alternatively, caspase-8 is also able to activate Bid, a pro-apoptotic member of the Bcl-2 family that triggers the release of cytochrome *c* from mitochondria (10, 11). Cytosolic cytochrome *c* forms a complex with Apaf-1 and activates caspase-9, the substrate of which is procaspase-3 (12). Then, the activated caspase-3 targets the DNA fragmentation factor, a heterodimeric protein complex consisting of the inhibitory chaperone protein DFF45 and the DFF40 nuclease (13). Cleavage of DFF45 by the protease results in the release of DFF40 from its inhibited state and allows nucleosomal DNA degradation, which is the ultimate stage of apoptosis (13–16). Both proteins of the DNA fragmentation factor complex share a homologous region at their N terminus called the CIDE-N (cell death-inducing DFF45-like effector) domain. This peculiar region, involved in the interaction between DFF40 and DFF45, is also found in the novel CIDE family of cell death activators (17). This common sequence explains the inhibitory control exerted by DFF45 on CIDE proteins, probably via homophilic interaction between their respective CIDE-N domains (17, 18). Proteins of this CIDE family differ from DFF40 by their specific C-terminal domain, called CIDE-C, which is responsible for their cell death property, which requires homodimerization and mitochondrial localization to fulfill their killing activity (17, 19).

Research on the impact of hepatitis C virus (HCV)[1] infection on host cell apoptosis is still hampered by the lack of a reliable cell culture system or of a small animal model that supports HCV replication and infection (20, 21). Thus, until now, few data have been obtained on possible strategies used by HCV to thwart apoptosis when used as an innate cellular antiviral defense. The HCV NS5A (nonstructural 5A) protein and the E2 (envelope 2) glycoprotein were recently proposed to directly interact and inhibit the enzymatic function of the interferon-induced double-stranded RNA-dependent PKR (22–24). This viral defense mechanism would prevent both protein synthesis inhibition, normally mediated by phosphorylation of eukaryotic

* This work was supported in part by INSERM and grants from the Ligue Nationale contre le Cancer (Comités d'Ille et Vilaine and Côte d'Armor). The costs of publication of this article were defrayed in part by the payment of page charges. This article must therefore be hereby marked "*advertisement*" in accordance with 18 U.S.C. Section 1734 solely to indicate this fact.

§ Postdoctoral Fellow of the Association pour la Recherche sur le Cancer. To whom correspondence should be addressed: INSERM U522, Hôpital de Pontchaillou, 2, rue Henri le Guilloux, 35033 Rennes Cedex, France. Tel.: 33-2-9954-3737; Fax: 33-2-9954-0137; E-mail: lars.erdtmann@univ-rennes1.fr.

¶ Supported by a scholarship from the Ministry of Culture, National Education, and Research of Luxembourg (reference number 01/20).

[1] The abbreviations used are: HCV, hepatitis C virus; GST, glutathione *S*-transferase; GFP, green fluorescent protein; Gal4BD, Gal4 DNA-binding domain; Gal4AD, Gal4 activation domain.

initiation factor 2-α (25), and apoptosis induced through the Fas-associated death domain-mediated death signaling pathway (3–5). The HCV core protein has been reported also to interfere with the Fas-mediated death signaling pathway. However, its role as an apoptosis enhancer or inhibitor is still in debate (26–32).

Interestingly, our investigations suggest that the HCV NS2 (nonstructural 2) protein intervenes in the viral defense system against apoptosis. Mature NS2 is a 23-kDa hydrophobic transmembrane protein anchored to the endoplasmic reticulum (33). It is generated by proteolytic processing of the HCV polypeptide in the infected cell (34). Although the biological relevance of NS2 in polypeptide processing was previously demonstrated by a study showing that a modified HCV genome (in which mutations were introduced into the NS2 sequence) encoded an HCV polypeptide that abolished its infectivity in chimpanzees (35), the biological function of the cleaved mature NS2 protein is still unknown.

In this study, we identified for the first time a cellular partner of NS2, the CIDE-B protein, a member of the recently identified pro-apoptotic CIDE family. We show that CIDE-B mediates cytochrome *c* release from mitochondria and caspase 3 activity and that NS2 acts as an inhibitor of CIDE-B-induced apoptosis. *In vivo*, CIDE-B was suppressed in adenovirus-infected transgenic mice expressing HCV proteins. We suggest that NS2 interferes with the CIDE-B-induced death pathway and participates in HCV strategies to subvert host cell defense.

EXPERIMENTAL PROCEDURES

Plasmid Constructions

Yeast Expression Vectors—The pAS2ΔΔ-NS3 and pAS2ΔΔ-NS4 vectors were a kind gift of P. Legrain (38, 50). The cloned HCV-H genome was provided by G. Inchauspé (51). The *NS2* gene was amplified from the HCV-H genome by PCR and subcloned into the *Nco*I and *Bam*HI sites of pAS2ΔΔ (50). Full-length CIDE-B and deletion mutants of NS2, NS3, and CIDE-B were amplified by PCR and inserted into the *Nco*I and *Bam*HI sites of vectors pAS2ΔΔ and pACT2 (Clontech, CA).

GST Expression Vectors—The *CIDE-B* gene was amplified by PCR from the pACT2-CIDE-B vector using a 5′-primer containing a *Bgl*II site that anneals upstream of the *Nco*I site within the pACT2 plasmid and a 3′-primer with an *Eco*RI site. The digested fragment was inserted in-frame with GST into the *Bam*HI and *Eco*RI sites of the pGEX4T1 plasmid (Amersham Biosciences). This cloning led to the introduction of two additional restriction sites, *Nco*I and *Bam*HI, which conferred to pGEX4T1 cloning compatibility with the yeast expression vectors. Thus, to generate the remaining GST vectors used in the cell-free assay, the *CIDE-B* gene was replaced with full-length NS2 or its deletion mutants or with mutant CIDE-B-(1–117) through direct subcloning from the yeast expression vectors into our modified pGEX4T1 vector (pGEX4T1-NB).

Mammalian Expression Vectors—NS2, NS2-(99–217), NS2-(140–217), or CIDE-B was subcloned into the *Kpn*I and *Eco*RI sites of the pEGFP-C3 plasmid (Clontech), yielding N-terminally tagged green fluorescent protein (GFP). The same sites were used to fuse NS2 to vesicular stomatitis virus G-tagged sequence in pVM6 (Roche Molecular Biochemicals) and CIDE-B to hemagglutinin-tagged sequence in pHM6 (Roche Molecular Biochemicals), yielding vectors pVM6-NS2 and pHM6-CIDE-B, respectively. The DFF45 vector was a kind gift of X. Wang (13). The *DFF45* gene was inserted in-frame with GFP, yielding the pEGFP-DFF45 vector. The pcDNA3-FLAG vector was a kind gift of G. Nunez (17). Full-length CIDE-B and its deletion mutants were inserted in-frame with FLAG downstream of the T7 promoter into the *Xba*I and *Apa*I sites of pcDNA3-FLAG. All DNA constructs were verified by DNA sequencing (Genome Express S. A.).[2]

Yeast Two-hybrid System

Two-hybrid screens were performed using the Gal4BD-NS2 or Gal4BD-NS2-(99–217) expression plasmid and the human liver cDNA library fused to Gal4AD in the pACT2 vector (HL4024AH, Clontech) according to the manufacturer's protocol. Interaction specificity was verified by a mating strategy as described previously (50). Positive clones were isolated, and interaction specificity was checked for a second time by a cotransforming approach (52). The cDNAs of clones that were positive in these two approaches were sequenced (Genome Express S. A.).

Random Mutagenesis by PCR and Screening of Mutants

The cDNA corresponding to C-terminal amino acids 110–219 of CIDE-B was amplified by error-prone PCR as described (39). Screening of the mutant library was performed as described previously (53) using Gal4BD-NS2-(99–217) as a bait.

Western Blot Analysis

GFP-expressing HeLa Cells—Cells were harvested in 20 μl of ice-cold lysis buffer (50 mM HEPES (pH 7.5), 150 mM NaCl, 1 mM EDTA, 2.5 mM EGTA, 0.1 Tween 20, 10% glycerol, 0.1 mM Na_3VO_4, 1 mM NaF, and 10 mM β-glycerophosphate with freshly added 0.1 mM phenylmethylsulfonyl fluoride, 10 mM dithiothreitol, and a protease inhibitor mixture tablet (Roche Molecular Biochemicals)). After 15 min, lysates were sonicated. Protein concentration was determined by the Bradford method (Bio-Rad), and 30 μg were subjected to 12.5% SDS-PAGE followed by Western blotting using anti-GFP antibody (Clontech).

Yeast Protein Extracts—Cells were harvested in 400 μl of 2× Laemmli buffer (Sigma) and vortexed in the presence of 400 μl of acid-washed glass beads (Sigma). The beads were spun down, and 20 μl of each protein sample were analyzed by Western blotting using anti-Gal4BD antibody LK5C1 (Santa Cruz Biotechnology, Santa Cruz, CA). All blots were treated with either horseradish peroxidase-labeled goat anti-rabbit or anti-mouse immunoglobulin (Dako Corp., Carpinteria, CA) and revealed using the SuperSignal kit (Pierce).

Production of Anti-human CIDE-B Antibody

A rabbit polyclonal antibody raised against a synthetic peptide mapping the N terminus of human CIDE-B (amino acids 5–19) was purchased from BioAtlantic (Nantes, France). The antibody was purified using the MabTrap kit (Amersham Biosciences) according to the manufacturer's instructions.

Binding Assays

Binding of NS2 to Recombinant CIDE-B—GST fusion proteins were expressed in *Escherichia coli* and purified as described (54). [^{35}S]Methionine-labeled CIDE-B and CIDE-B-(118–219) proteins were produced from their appropriate pcDNA3-FLAG vectors using the TnT T7 coupled reticulocyte lysate system (Promega, Madison, WI). Two micrograms of each purified GST protein were incubated overnight at 4 °C with 10 μl of ^{35}S-labeled CIDE-B or CIDE-B-(118–219) in phosphate-buffered saline containing 1 mM phenylmethylsulfonyl fluoride and protease inhibitors. Beads were washed five times with 10 mM Tris-HCl (pH 8.0), 1 mM EDTA, 150 mM NaCl, and 0.1% Tween 20 prior to their loading on SDS-polyacrylamide gels, and bound labeled materials were visualized by autoradiography.

Binding of NS2 to Human Endogenous Cellular CIDE-B—HepG2 cells were lysed and incubated with the different purified recombinant GST proteins as previously described (55). Human endogenous CIDE-B was detected with purified anti-CIDE-B antibody.

Cell Lines and Transfection

HeLa and COS-7 cells and the HepG2 human hepatoma cell line were cultured as described (52). For colocalization studies and analysis of cytochrome *c* release, cells were transfected by electroporation as described (52). For apoptosis assays, cells were transfected using the LipofectAMINE PLUS reagent kit (Invitrogen) according to the manufacturer's instructions.

Indirect Immunofluorescence

Twenty-four hours after electroporation, cells were treated as previously described (52). For FLAG-CIDE-B staining, permeabilized cells were incubated for 1 h with anti-FLAG antibody M2 (Sigma) diluted in phosphate-buffered saline with 0.2% saponin and 1% bovine serum albumin, washed, and then treated for 45 min with Texas Red-conjugated anti-mouse IgG (Jackson ImmunoResearch Laboratories, Inc., West Grove, PA). Cells were washed, mounted on a microscope slide with fluorescent mounting medium (Dako Corp.), and analyzed by confocal microscopy using a Leica TCS NT instrument.

[2] Detailed information about the primers used to amplify the different coding sequences are available upon request.

Cell Death Assay

HeLa cells (5×10^5) were spread on glass coverslips and transfected with 4 μg of the indicated mammalian expression vectors using the LipofectAMINE PLUS reagent kit. Twenty-four hours later, cells were fixed, and nuclei were stained for 15 min at room temperature with 0.5 μg/ml Hoechst 33342 (Sigma) in phosphate-buffered saline containing 0.5% saponin. Cells were washed and covered with microscope slides with the mounting medium, and apoptotic nuclei were identified on the basis of condensed chromatin and nuclear fragmentation using a Leica DM RXA instrument. Optical sections were mounted using Adobe Photoshop software.

Analysis of Mitochondrial Release of Cytochrome c

HeLa cells (2.4×10^7) were transfected with 25 μg of the indicated mammalian expression vectors. After 24 h, mitochondria were isolated. Briefly, cells were collected, washed, and resuspended in fractionation buffer containing 250 mM sucrose, 20 mM Tris-HCl (pH 8.0), 1 mM EDTA, 1 mM dithiothreitol, 1 mM phenylmethylsulfonyl fluoride, and a protease inhibitor mixture tablet. Cells were homogenized in a Dounce glass homogenizer (B pestle) and centrifuged at $1000 \times g$ for 10 min at 4 °C to remove intact cells and nuclei. Supernatants were centrifuged at $10{,}000 \times g$ for 25 min at 4 °C to separate mitochondrial and cytosolic fractions. The mitochondrial pellet was resuspended in 20 μl of fractionation buffer, and protein concentration were determined by the Bradford method. A total of 30 μg of mitochondrial protein were subjected to 15% SDS-PAGE followed by Western blotting using anti-cytochrome *c* antibody H104 (Santa Cruz Biotechnology).

To immunoprecipitate cytosolic cytochrome *c*, 800 μg of protein issued from each cytosolic fraction were incubated for 3 h at 4 °C with anti-cytochrome *c* antibody 6H2.B4 (Pharmingen) and 30 μl of protein A-Sepharose beads (Amersham Biosciences). The beads were washed, and bound cellular proteins were analyzed by Western blotting using anti-cytochrome *c* antibody H104.

Caspase Activity Assay

COS-7 cells were transfected with 2 μg of pEGFP or pHM6-CIDE-B vector, harvested at 24 h, and lysed in caspase activity buffer (56). One-hundred micrograms of crude cell lysate were incubated with 80 μM substrate-7-amino-4-methylcoumarin for 1 h at 37 °C. Caspase-mediated cleavage of DEVD-7-amino-4-methylcoumarin was measured by spectrofluorometry (Molecular Devices) at an excitation/emission wavelength pair of 380/440 nm. Caspase activity is indicated in V_{max} values.

HCV Transgenic Mice

Transgenic mice with liver-specific expression of RNA encoding the complete viral polyprotein were produced as described (42).

Adenoviral Infections and β-Galactosidase Assays

Mice were infected with 2.5×10^9 plaque-forming units of adenoviral β-galactosidase (Rous sarcoma virus-β-galactosidase) (57) by tail intravenous injections. Liver biopsies were collected 21 days post-infection. Crude protein extract from 0.5 μg of liver powder was tested for β-galactosidase activity using the luminescent β-galactosidase assay (Clontech) according to the manufacturer's instructions.

Liver protein extracts were analyzed by 12% SDS-PAGE followed by Western blotting using anti-CIDE-B antibody E-19 (Santa Cruz Biotechnology). To ensure comparable loading of the samples, the blot was incubated with anti-annexin V antibody (kind gift of F. Russo-Marie). Specific bands were quantified by scanning the autoradiographs with a Shimadzu densitometer.

Data Analysis

Statistical analysis was performed using Student's *t* test for unpaired data. Data were considered to be significant at $p < 0.05$ and $p < 0.01$.

RESULTS

Identification of CIDE-B as a Cellular Partner of NS2—Mature HCV NS2 is a viral protein of unknown function. To elucidate its biological role, we searched for possible cellular protein partner(s) that directly interact with NS2 using the two-hybrid system. Full-length NS2 was used as a bait to screen a human liver cDNA library. Although Western blot analysis showed expression of the bait (Fig. 1*A*, *lane 3*), no specific interaction could be detected (data not shown). This

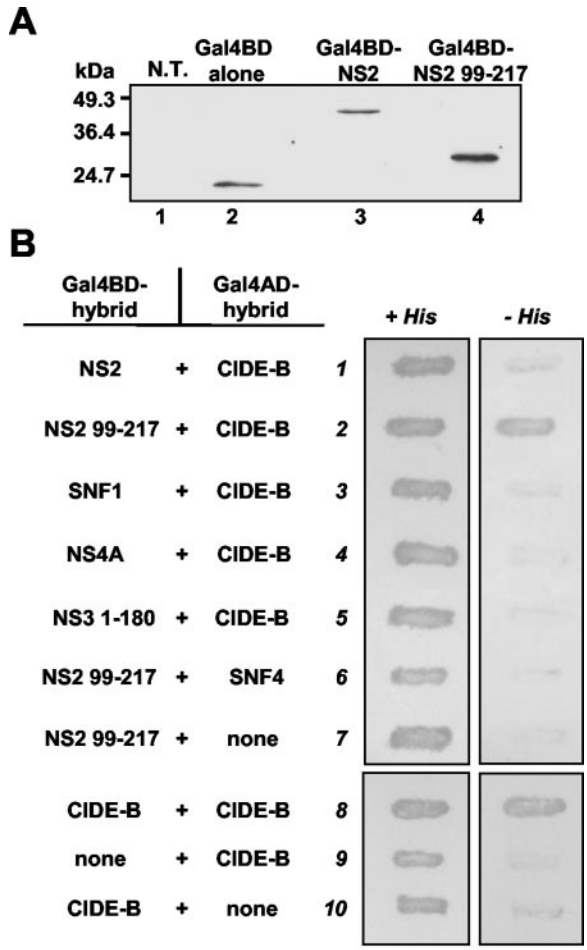

FIG. 1. **Specific interaction of the HCV NS2 C terminus with the human CIDE-B protein in the two-hybrid system.** *A*, shown are the results from Western blot analysis of the different bait proteins. Yeast extracts were prepared from the AH109 yeast strain transformed with each of the indicated Gal4BD hybrid proteins (*lanes 2–4*) and analyzed using anti-Gal4BD antibody. *Lane 1* contains non-transfected (*N.T.*) cells. *B*, the AH109 reporter yeast strain expressing the pairs of indicated hybrid proteins fused to Gal4BD and Gal4AD was analyzed for histidine auxotrophy. AH109 double transformants were patched on medium containing histidine (*+His*) and then replica-plated on histidine-free medium (*−His*). Yeast growth in the absence of histidine indicates interaction between hybrid proteins. For the mutant NS2-(99–217), the hydrophobic region at the N terminus of NS2 from amino acids 1–98 was omitted (corresponding to amino acids 810–908 in the HCV polypeptide). Binding specificity was assessed using different yeast (SNF1 and SNF4) and viral (NS4A and NS3-(1–180)) proteins (*rows 3–6*). The known homodimerization of human CIDE-B was used as a positive binding control (*lane 8*).

observation may be explained by the presence of hydrophobic and transmembrane domains at the N terminus of NS2 (amino acids 1–98) (33, 36, 37), which might hamper the nuclear translocation of the bait, thus preventing the detection of any interaction. Therefore, we performed a second two-hybrid screen using an NS2 mutant with residues 1–98 deleted (NS2-(99–217)) (*lane 4*). A 1.2-kb cDNA encoding human CIDE-B, a protein of 219 amino acids, could be isolated. We further examined the interaction specificity between CIDE-B and NS2 (Fig. 1*B*). First of all, background binding was excluded using empty constructs (*rows 7*, *9*, and *10*). Because CIDE-B has also been shown to homodimerize (19), this property was used to check the functional integrity of this cloned CIDE-B (*row 8*). CIDE-B specifically bound to NS2-(99–217) (*row 2*); but, as expected, no interaction could be revealed when the hydrophobic N terminus was maintained in the NS2 sequence, probably for the reasons explained above. Any unspecific binding with

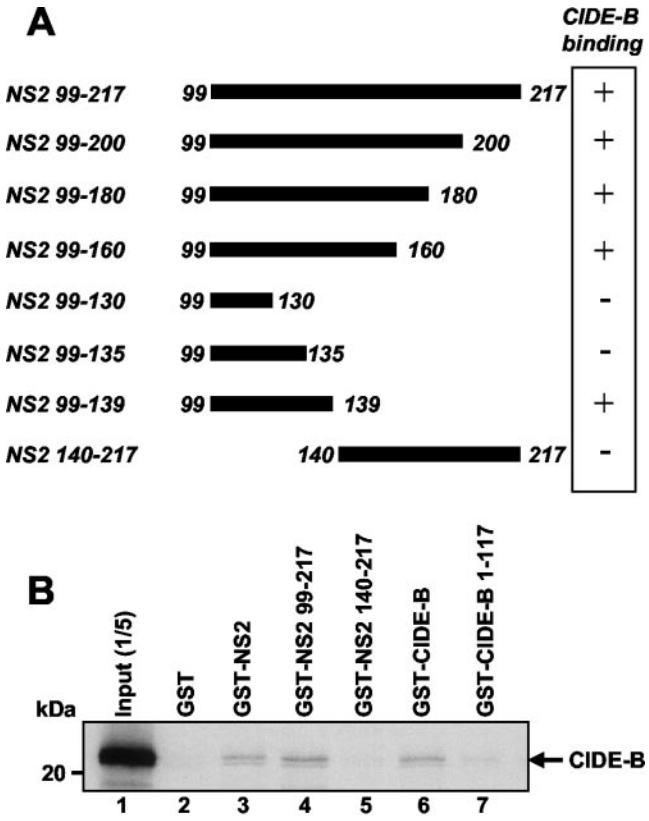

FIG. 2. **Characterization of NS2 binding to human CIDE-B.** *A*, mapping of the NS2 domain interacting with CIDE-B in the two-hybrid assay. The AH109 yeast strain was cotransformed with Gal4AD-CIDE-B and each Gal4BD-NS2 deletion mutant. The N- and C-terminal extremities of each NS2 deletion mutant are indicated by *numbers* corresponding to the amino acid positions in the NS2 sequence. AH109 double transformants were analyzed for histidine auxotrophy. A *plus sign* indicates transactivation of the reporter gene (*HIS3*). *B*, interaction of full-length NS2 and its mutants expressed as GST fusion proteins with the CIDE-B protein in a cell-free assay. *In vitro* translated ^{35}S-labeled CIDE-B was incubated with equal amounts of purified GST (*lane 2*), GST-NS2 (full-length) (*lane 3*) or GST-fused truncated recombinant NS2 proteins (*lanes 4* and *5*), previously immobilized on glutathione-agarose beads. Bound labeled material was analyzed by SDS-PAGE and autoradiography. Immobilized GST-fused full-length (*lane 6*) and truncated (*lane 7*) CIDE-B proteins were used as binding controls. One-fifth of the ^{35}S-labeled CIDE-B input for the binding assay was run in *lane 1*.

CIDE-B was excluded because no interaction was detected either between CIDE-B and an unrelated protein such as Snf1 (*row 3*) or between CIDE-B and other viral proteins such as NS4A and NS3-(1–180) (*rows 4* and *5*, respectively). We preferentially used the N-terminal proteinase domain (NS3-(1–180)) because it was already identified as a valuable prey in a two-hybrid screen carried out with NS4A as a bait (38). Finally, no interaction was detected between NS2-(99–217) and Snf4, a non-relevant yeast protein (*row 6*). Taken together, our results provide evidence that the human CIDE-B protein is a specific cellular partner of the viral NS2 protein.

Characterization of the NS2 Region Involved in Binding to CIDE-B—To define the region within NS2 involved in the interaction with CIDE-B, we tested different truncation mutants of NS2-(99–217) for their capacity to bind CIDE-B in the two-hybrid system. The results shown in Fig. 2*A* indicate that at least a region encompassing amino acids 135–139 of NS2 supports interaction with CIDE-B.

The data obtained in the two-hybrid system were confirmed by a biochemical approach (Fig. 2*B*). Polypeptides of full-length NS2 and CIDE-B and their deletion mutants were produced as recombinant GST fusion proteins and immobilized on glutathione-agarose beads. The different GST proteins were tested for their ability to retain *in vitro* translated ^{35}S-labeled CIDE-B. Whereas no background binding could be detected on the GST protein (*lane 2*), ^{35}S-labeled CIDE-B was retained on GST-CIDE-B (*lane 6*). This result validates the system because it reproduced the known homodimerization of the cellular protein. Moreover, CIDE-B with its C terminus deleted (GST-CIDE-B-(1–117)) lost its capacity to dimerize with the wild-type form of the protein (*lane 7*), a result that is thus consistent with the observation that the C-terminal domain is required for CIDE-B dimerization (19). Interestingly, this cell-free methodology allowed us to highlight that both the truncated (NS2-(99–217)) (*lane 4*) and full-length (*lane 3*) NS2 proteins have the identical property of binding to CIDE-B. These data support our hypothesis given above that the lack of interaction observed in the two-hybrid screen with wild-type NS2 is not due to the inability of the viral protein to bind to CIDE-B, but instead to the presence of its hydrophobic domains which are unsuited for this methodology. Furthermore, GST-NS2-(140–217) did not retain labeled CIDE-B (*lane 5*), consistent with our results obtained in the two-hybrid experiment.

The CIDE-B C-terminal Domain Is Required for Both Homodimerization and NS2 Binding—To determine the domain in CIDE-B required for NS2 binding, we generated two deletion mutants: (i) CIDE-B-(1–117), which contains the CIDE-N domain sharing homology with the N-terminal regions of DFF40 and DFF45, and (ii) CIDE-B-(118–219), which comprises the CIDE-C domain sufficient for CIDE-B dimerization and death activity (Fig. 3*A*) (17). Both deletion mutants were fused to Gal4AD and analyzed for their binding capacity with Gal4BD-CIDE-B and Gal4BD-NS2-(99–217) in the AH109 yeast strain. Gal4BD-NS2-(140–217) was added as a negative control (Fig. 3*B*, *row 4*). CIDE-B homodimerization, highlighted by the interaction between the full-length proteins (*row 5*), was maintained only with the deletion form containing the C-terminal domain of the protein (*rows 6* and *7*). This domain was revealed to be also involved in the binding to NS2-(99–217) because its presence was required for the interaction with the viral protein (*rows 1–3*).

We attempted to corroborate these findings with the cell-free binding assay, which also permitted testing of full-length NS2. The retention of *in vitro* translated ^{35}S-labeled CIDE-B-(118–219) was tested against different recombinant GST proteins (Fig. 3*C*). CIDE-B-(118–219) was adsorbed only on beads displaying either full-length CIDE-B (*lane 6*) or NS2 containing residues 99–139 (*lanes 3* and *4*), whereas no interaction was revealed for GST, GST-NS2-(140–217), or GST-CIDE-B-(1–117) (*lanes 2*, *5*, and *7*, respectively).

To identify precisely the residues involved in NS2 binding, we randomly mutagenized CIDE-B C-terminal amino acids 110–219 by error-prone PCR (39), and we searched for mutants unable to interact with NS2-(99–217) in the two-hybrid system. We isolated a CIDE-B C-terminal mutant whose interaction with NS2-(99–217) was impaired by a single point mutation (Fig. 3*D*, *row 2*). This mutant contains phenylalanine instead of tyrosine at position 160 (Y160F). Interestingly, this CIDE-B mutant also failed to interact with native CIDE-B (*row 4*), illustrating that CIDE-B homodimerization is impaired in yeast cells. Taken together, these results indicate that the CIDE-B C-terminal domain seems to be sufficient for both CIDE-B dimerization and NS2 interaction.

NS2 Associates with CIDE-B in the Cell—We further investigated the subcellular localization of NS2 and CIDE-B by immunofluorescence staining and confocal microscopy analysis in mammalian cells. NS2 and its deletion mutants were ex-

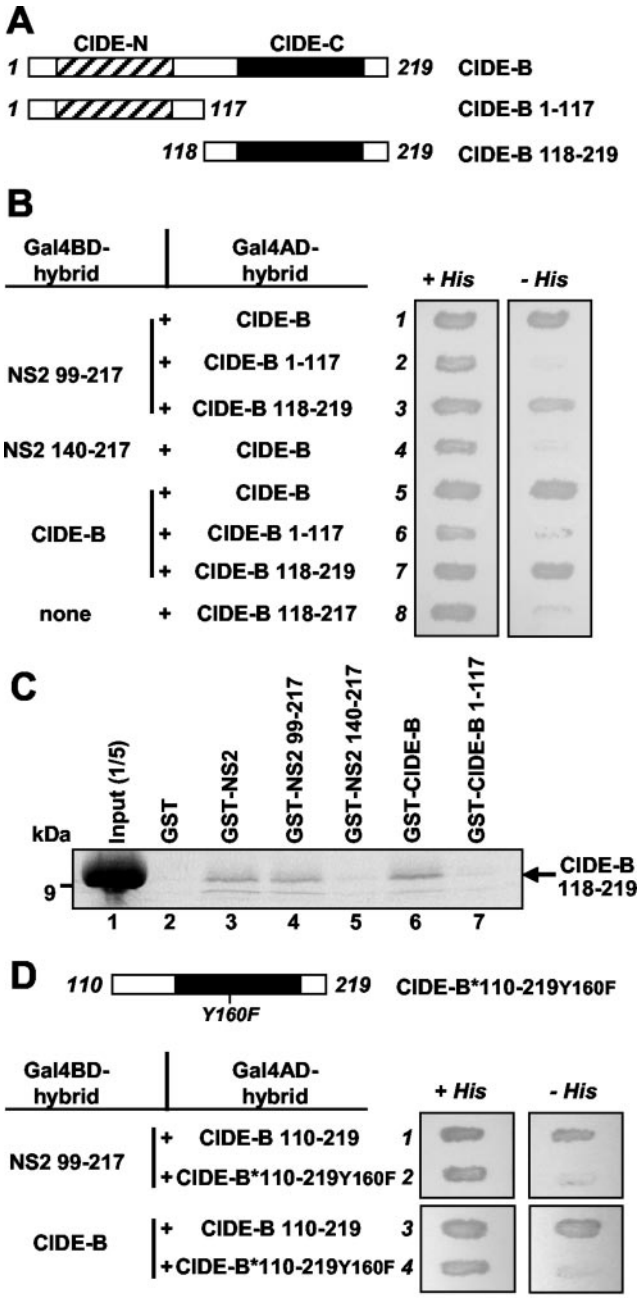

FIG. 3. **Identification of the NS2-binding domain in the human CIDE-B protein.** *A*, schematic representation of the CIDE-B protein and its deletion mutants. The CIDE-N and CIDE-C domains are represented as *gray* and *black boxes*, respectively. *B*, mapping of the CIDE-B domain interacting with the NS2 C terminus in the two-hybrid assay. The AH109 reporter yeast strain expressing the pairs of indicated hybrid proteins fused to Gal4BD and Gal4AD was analyzed as described in the legend to Fig. 1*A*. The AH109 yeast strain cotransfected with Gal4BD-CIDE-B and each of the indicated Gal4AD hybrid proteins (*rows 5–7*) was used as binding controls. *C*, binding of CIDE-B-(118–219) to GST-fused full-length and truncated NS2 proteins in a cell-free assay. *In vitro* translated ^{35}S-labeled CIDE-B-(118–219) (*lanes 2–7*) was incubated with equal amounts of the different purified GST fusion proteins as described in the legend to Fig. 2*B*. Bound labeled material was analyzed by SDS-PAGE and autoradiography. Immobilized GST-fused full-length (*lane 6*) and truncated (*lane 7*) CIDE-B proteins were used as binding controls. One-fifth of the ^{35}S-labeled CIDE-B-(118–219) input for the binding assay was run in *lane 1*. *D*, identification of a CIDE-B C-terminal mutant deficient for NS2 interaction. Shown is a schematic representation of the CIDE-B-(110–219)Y160F mutant. The CIDE-B C-terminal cDNA was randomly mutagenized by error-prone PCR, and the mutants unable to interact with NS2-(99–217) were analyzed by DNA sequencing. The interaction of the CIDE-B-(110–219)Y160F mutant with NS2 and CIDE-B was analyzed as described for *B*.

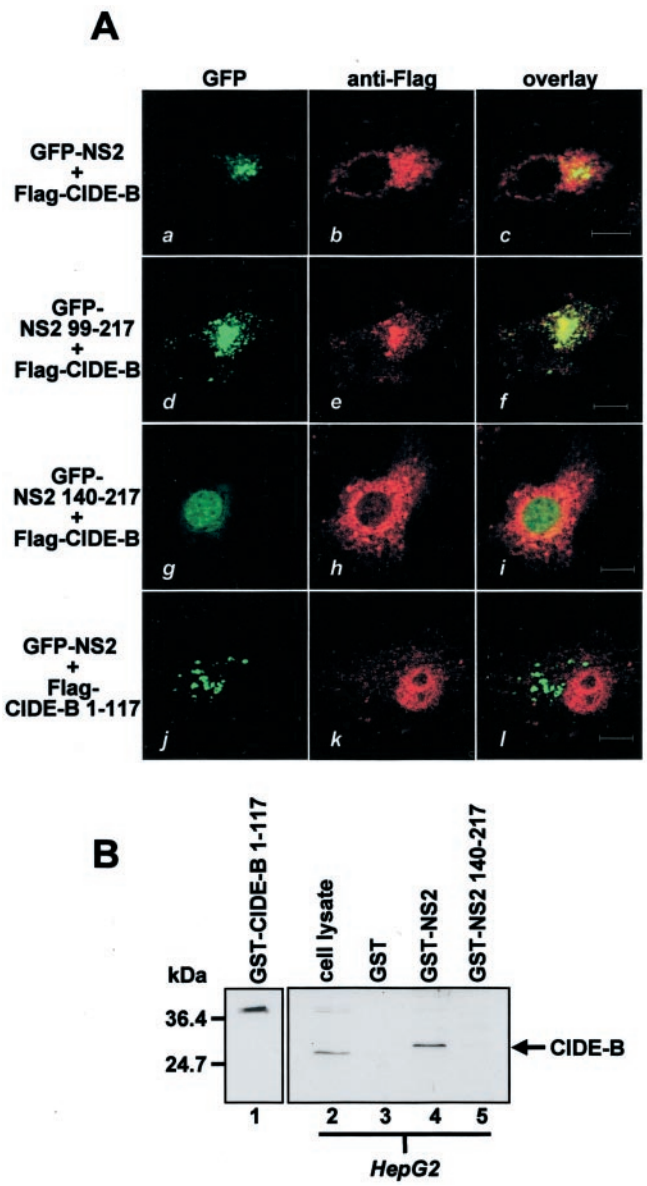

FIG. 4. **NS2 associates with CIDE-B in the cell.** *A*, HeLa cells were cotransfected with 12 μg of pcDNA3-FLAG-CIDE-B or pcDNA3-FLAG-CIDE-B-(1–117) along with 12 μg of the different GFP vectors (*panels a*, *d*, *g*, and *j*). After 24 h, cells were fixed, permeabilized, treated with anti-FLAG monoclonal antibody, and stained with a Texas Red-conjugated Fab fragment recognizing mouse IgG. Subcellular localization of GFP proteins (*panels a*, *d*, *g*, and *j*) and FLAG-tagged proteins (*panels b*, *e*, *h*, and *k*) was analyzed by confocal microscopy, and colocalization was visualized by overlay (*panels c*, *f*, *i*, and *l*). *B*, shown is the binding of NS2 to endogenous CIDE-B. HepG2 lysates were incubated with equal amounts of purified GST (*lane 3*), GST-NS2 (*lane 4*), and GST-NS2-(140–217) (*lane 5*). Bound proteins were resolved by SDS-PAGE, and CIDE-B association was analyzed by Western blotting. Purified GST-CIDE-B-(1–117) (*lane 1*) and crude cell lysate (*lane 2*) were used as controls for specific anti-CIDE-B antibody recognition. *Scale bar*, 10 μm.

pressed as GFP chimeras, whereas wild-type and truncated CIDE-B proteins were FLAG-tagged at their N termini. Cells were cotransfected with the different plasmids as indicated in Fig. 4. After 24 h, GFPs were revealed by direct GFP fluorescence, and the cellular distribution of CIDE-B was examined by staining with an antibody directed against the FLAG epitope.

As previously described (19), FLAG-CIDE-B showed a punctate signal, with the presence of discrete dots in a perinuclear region (Fig. 4, *panels b*, *e*, and *h*). We detected full-length NS2 fused to GFP in the perinuclear space (see Fig. 5*B*, *panel b*), as

reported by Kim *et al.* (40). Coexpression of CIDE-B and the NS2 chimera revealed partial overlapping staining signals in the perinuclear region, indicating that fractions of both proteins were located in the same area (Fig. 4*A*, *panel c*). Interestingly, the recombinant GFP-NS2-(99–217) protein, corresponding to the deletion mutant used as a bait protein in the two-hybrid screen, showed a localization pattern similar to that of the full-length protein (*panels a* and *d*) and still colocalized with CIDE-B (*panel f*). In contrast, the subcellular localization of the GFP-NS2-(140–217) chimera, comprising the deletion mutant deficient for CIDE-B *in vitro* binding, lost the dense localization of GFP-NS2 and GFP-NS2-(99–217). GFP-NS2-(140–217) was mostly found in the nucleus, and a weak diffuse signal was also detected in the cytoplasm (*panels g* and *i*). Notwithstanding, the subcellular distribution of FLAG-CIDE-B was maintained in part of the perinuclear space (*panel h*). The deletion mutant FLAG-CIDE-B-(1–117), defective for both dimerization and NS2 binding, showed diffuse cytoplasmic staining, with a significant fraction accumulating in the nucleus (*panel k*). Therefore, no overlapping staining signal with GFP-NS2 was observed (*panel l*).

Because we could not exclude in these experiments that the observed colocalization patterns were due to the ability of two overexpressed proteins to form aggregates in the cell, we further investigated the interaction of NS2 with endogenous CIDE-B. For this purpose, we developed a novel antibody raised against a synthetic peptide mapping the N terminus of human CIDE-B (amino acids 5–19). As expected, this antibody recognized purified GST-CIDE-B-(1–117), as demonstrated in Fig. 4*B* (*lane 1*). To determine whether NS2 associates with endogenous CIDE-B, we incubated HepG2 lysates with purified GST, GST-NS2, or GST-NS2-(140–217) immobilized on glutathione-agarose beads. Bound proteins were analyzed by Western blotting with anti-CIDE-B antibody. Endogenous CIDE-B bound to GST-NS2 (*lane 4*), but not to GST (*lane 3*) or GST-NS2-(140–217) (*lane 5*), the deletion mutant deficient for CIDE-B interaction in the two-hybrid system (Fig. 2*B*).

NS2 Inhibits CIDE-B-induced Apoptosis—Because CIDE-B is involved in apoptosis, it was important to study whether NS2 binding to CIDE-B could interfere with the death signal mediated by CIDE-B. We analyzed the apoptotic state of cells transfected with GFP-CIDE-B along with either a non-relevant protein (β-galactosidase) or GFP-fused full-length or truncated NS2 (Fig. 5*A*). The morphological features of apoptosis in GFP-positive adherent cells were evaluated after nuclear Hoechst staining. The percentage of apoptotic cells (identified by condensed nuclei and fragmented chromatin) was calculated against the total number of GFP-positive cells. Typical apoptotic and live cells are shown in Fig. 5*B* (*panels a* and *b*, respectively). Whereas GFP alone had only a weak apoptotic background activity (15%) (Fig. 5*A*), GFP-CIDE-B induced cell death in ~60% of transfected cells, a level previously observed by others (19). As a control, we used GFP-fused DFF45, which is known to be a specific cellular inhibitor of CIDE-B (17). DFF45, NS2, NS2-(99–217), and NS2-(140–217), each fused to GFP and transfected individually, generated an apoptotic background comparable to that obtained with GFP alone. Interestingly, cells coexpressing GFP-CIDE-B and GFP-NS2 or GFP-NS2-(99–217) were partially protected from CIDE-B-induced apoptosis (~30%) at a level similar to that observed for cells coexpressing GFP-CIDE-B and GFP-DFF45. By contrast, cells coexpressing GFP-NS2-(140–217), which was demonstrated to be deficient for CIDE-B *in vitro* binding, did not affect CIDE-B-induced apoptosis. The correct expression of all GFP chimeras used was verified by Western blot analysis, excluding that the absence of inhibition observed for GFP-NS2-(140–217) was due to a lack of protein expression (Fig. 5*C*). These results suggest a striking correlation between the ability of NS2 and its deletion mutants to bind to CIDE-B and to inhibit CIDE-B-induced apoptosis, suggesting that the interaction of NS2 with CIDE-B interferes with the death signal mediated by CIDE-B.

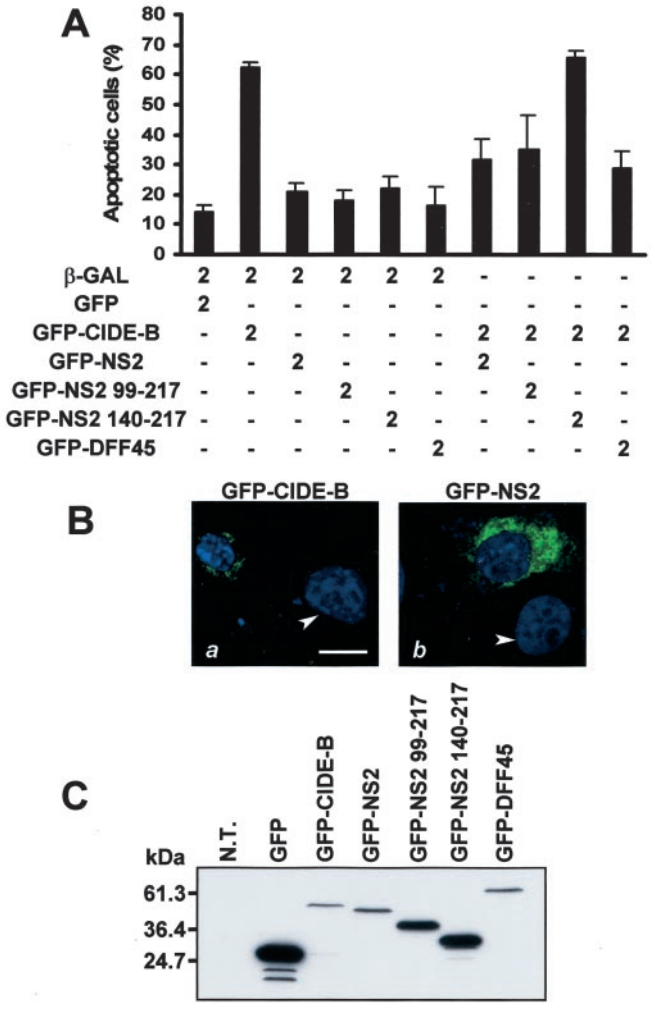

FIG. 5. **The NS2 protein inhibits CIDE-B-induced apoptosis.** *A*, quantification of apoptotic GFP-positive adherent cells. HeLa cells were cotransfected with the indicated amounts (0 or 2 μg) of different mammalian expression vectors. After 24 h, cells were stained with Hoechst 33342 and observed under a fluorescence microscope. Apoptotic GFP-expressing cells with condensed nuclei and fragmented chromatin were counted, and the percentage of cell death was calculated against the total number of GFP-positive cells (n = 150). *Error bars* represent means ± S.D. of three independent experiments. *B*, nuclear morphological analysis of GFP-positive adherent cells. HeLa cells were treated as described for *A*. The nuclear morphology of non-transfected non-apoptotic cells is indicated by *white arrows*. *Scale bar* = 10 μm (magnification × 800). *C*, Western blot analysis. Lysates from cells expressing the indicated GFP fusion proteins were analyzed using anti-GFP antibody. *β-GAL*, β-galactosidase; *N.T.*, non-transfected cells.

NS2 Interferes with the Mitochondrial Cytochrome c Release Induced by CIDE-B—Although it was reported that mitochondrial localization and dimerization are required for CIDE-B to induce cell death (19), the precise apoptotic mechanism remained unknown. We wondered whether CIDE-B might be involved in the mitochondrial death pathway and thus might induce apoptosis in a caspase-dependent manner (for review, see Ref. 41). We first studied whether CIDE-B induces caspase-3 activity. Fig. 6*A* shows that the V_{max} values of CIDE-B-expressing cells were 3-fold higher than those of GFP-expressing control cells, indicating enzymatic activity of caspase-3 in the presence of CIDE-B.

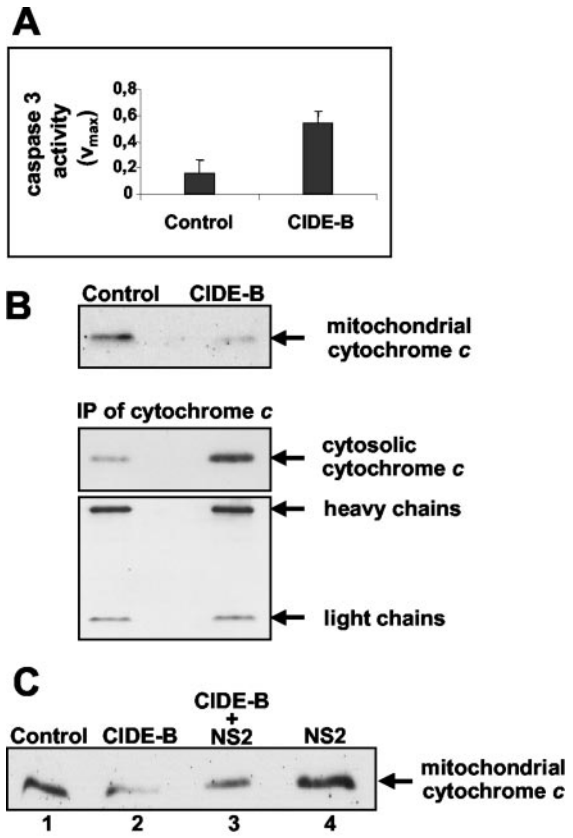

FIG. 6. **NS2 prevents CIDE-B-induced apoptosis in mitochondria.** *A*, CIDE-B induces caspase activity. Cells were transfected with 2 μg of pEGFP or pHM6-CIDE-B vectors. After 24 h, cell lysates were assayed for caspase-3 activity. Enzymatic activity is indicated in V_{max} values. *B*, CIDE-B induces cytochrome *c* release from mitochondria. HeLa cells were transfected with 20 μg of pcDNA3 (control) or pcDNA3-FLAG-CIDE-B vector. After 24 h, cells were homogenized, and mitochondrial and cytosolic fractions were prepared. Thirty micrograms of each mitochondrial fraction were subjected to Western blotting using anti-cytochrome *c* antibody H104 (*upper panel*). Cytochrome *c* released in cytosolic fractions was immunoprecipitated with equal amounts of anti-cytochrome *c* antibody 6H2.B4 prior to Western blot analysis (*middle panel*). Immunoprecipitation (*IP*) was standardized by the detection of the heavy and light chains of the anti-cytochrome *c* antibody used (*lower panel*). *C*, NS2 inhibits CIDE-B-induced cytochrome *c* release from mitochondria. Cells were cotransfected with 5 μg of pcDNA3 or pcDNA3-FLAG-CIDE-B along with 20 μg of pVM6-NS2 or pcDNA3 vector. Equal amounts of mitochondrial fractions were analyzed by Western blotting. *Control*, mitochondrial fraction of non-transfected cells.

Because caspase-3 activity can be the result of cytochrome *c* release from mitochondria during apoptosis (for review, Ref. 41), we further wondered whether CIDE-B could be associated with the cytochrome *c* release. For this investigation, we prepared mitochondrial and cytosolic fractions from HeLa cells transfected with either an empty plasmid or a recombinant plasmid expressing CIDE-B. Cytochrome *c* was directly detected by Western blotting in the mitochondrial fraction or was first immunoprecipitated from the cytosolic fraction. Obviously, as shown in Fig. 6*B*, CIDE-B induced cytochrome *c* release as shown by the decreased amount of cytochrome *c* detected in the mitochondrial fraction and its increased level observed in the cytosolic fraction of the CIDE-B-expressing cells compared with the control cells. These results demonstrate that CIDE-B-induced apoptosis is accompanied by cytochrome *c* release.

We further wondered whether NS2 counteracts the cytochrome *c* release induced by CIDE-B to protect cells from apoptosis. To answer this question, we assessed the mitochondrial cytochrome *c* levels in HeLa cells transiently transfected with FLAG-tagged CIDE-B or vesicular stomatitis virus G-tagged NS2 or cotransfected with both proteins (Fig. 6*C*). The signal revealed in cells expressing vesicular stomatitis virus G-tagged NS2 (*lane 4*) was comparable to that obtained in the control cells (*lane 1*), whereas only a weak band was detected in mitochondria isolated from FLAG-CIDE-B-expressing cells (*lane 2*). When CIDE-B and NS2 were coexpressed (*lane 3*), cytochrome *c* release was partly avoided because the signal intensity was intermediate to those detected in the control (*lane 1*) and CIDE-B-expressing (*lane 2*) cells. This result suggests that NS2 may protect cells from the cytochrome *c* release induced by the apoptotic CIDE-B protein.

CIDE-B Expression Is Sensitive to Viral Infection, and Its Protein Content Is Altered in HCV Transgenic Mice—To examine whether CIDE-B expression is sensitive to HCV proteins *in vivo*, we used a previously described HCV transgenic mice model (42) that permits the study of NS2 activity within the context of the entire viral polyprotein rather than in isolation. Indeed, interactions between viral proteins can significantly modulate their effects *in vivo* (42) and thus explain the conflicting results obtained in transgenic mice expressing single HCV proteins (43).

We first analyzed the CIDE-B protein content in liver tissues from wild-type and HCV transgenic mice by Western blotting. Fig. 7 (*A* and *B*) shows that the CIDE-B protein content was similar between HCV transgenic and wild-type mice. Because HCV proteins in the transgenic mice are not recognized as foreign proteins inducing an immune response, we decided to analyze the CIDE-B protein content in the context of viral infection. We compared the CIDE-B protein content in liver extracts from non-transgenic and HCV transgenic mice, both infected with an adenovirus. As shown in Fig. 7 (*C* and *D*), the amount of CIDE-B in the livers of adenovirus-infected wild-type mice was reduced to 35% of that in the livers of normal mice. Interestingly, when the HCV transgenic mice were infected with an adenovirus, the CIDE-B protein level was dramatically lowered to 1% of that in wild-type mice.

DISCUSSION

Chronic HCV infection frequently leads to liver cancer. Because the liver is the major HCV replication site, HCV seems to have developed strategies to promote its survival in this organ. This study points out the interaction between the viral NS2 protein and liver-specific CIDE-B, a cellular protein involved in apoptosis, as a mechanism contributing to the prevention of apoptosis. The interaction of NS2 with CIDE-B was evidenced by yeast two-hybrid and cell-free assays associated with colocalization studies and coprecipitation experiments of human endogenous CIDE-B. The NS2-binding site was determined to be the CIDE-B cell death domain. This binding is sufficient to inhibit CIDE-B-induced apoptosis because an NS2 deletion mutant unable to interact with CIDE-B *in vitro* lost its capacity to interfere with CIDE-B cell death activity. Additional interest is provided by the binding specificity for CIDE-B. Indeed, CIDE-A, the second member of the CIDE protein family, which presents a widespread tissue distribution except in the liver (17), does not bind to NS2 (data not shown).

The pro-apoptotic CIDE-B protein can be divided into two distinct domains: the N-terminal (CIDE-N) and C-terminal (CIDE-C) domains. The CIDE-N domain shares homology with the N-terminal regions of DFF40 and DFF45, a nuclease and its inhibitor, respectively. The CIDE-B C-terminal region is necessary and sufficient for the intrinsic apoptotic activity of CIDE proteins (17). Interestingly, we determined that the interaction of NS2 takes place within the CIDE-B C-terminal domain, whereas this domain is also involved in the ho-

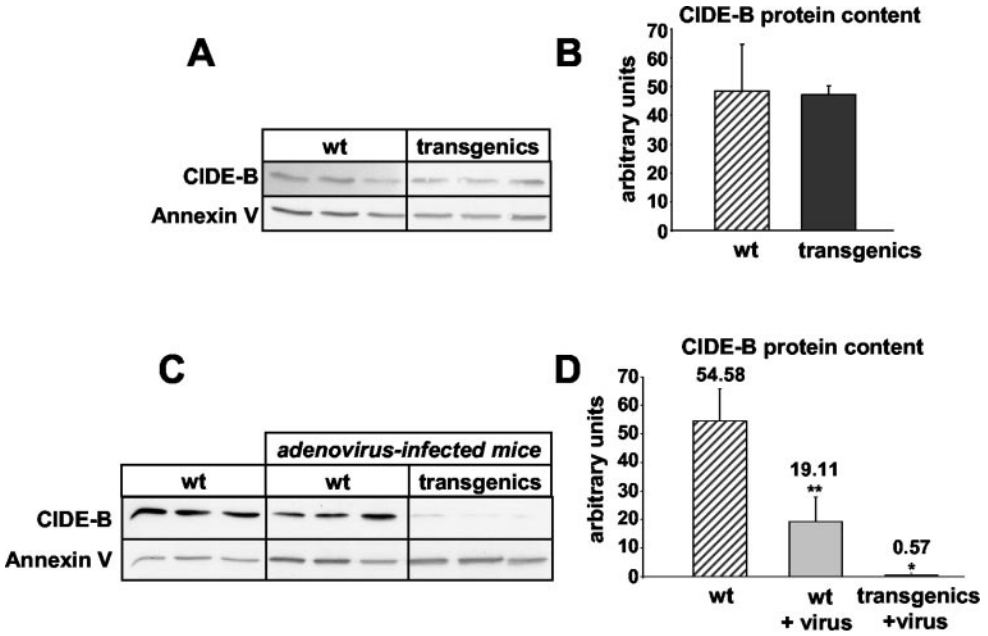

FIG. 7. **CIDE-B protein content in the livers of HCV transgenic mice compared with wild-type mice without and with adenoviral infection.** *A*, Western blot analysis was performed with 45 μg of liver extract from animals using anti-CIDE-B and anti-annexin V antibodies. *B*, quantitated results are expressed as means ± S.D. of five HCV transgenic and five wild-type (*wt*) mice. The values obtained with the HCV transgenic mice are not statistically different from those obtained with the wild-type mice ($p = 0.8864$). *C*, Western blot analysis was performed as described for *A*. *D*, quantitated results are expressed as means ± S.D. of five wild-type mice, and five adenovirus-infected wild-type mice, and five adenovirus-infected HCV transgenic mice. The values obtained with the virus-infected wild-type mice are statistically different from those obtained with the wild-type mice ($p = 0.0041$) and the virus-infected HCV transgenic mice ($p = 0.0132$). *, $p < 0.05$; **, $p < 0.01$.

modimerization of CIDE-B (this study and Ref. 19). In addition, tyrosine 160 in the CIDE-B C-terminal domain is necessary for both CIDE-B dimerization and NS2 interaction, suggesting a putative binding competition between NS2 and CIDE-B for CIDE-B itself. Because homodimerization is required for CIDE-B cell death activity, we suggest that NS2 binding might affect CIDE-B-induced apoptosis by interfering with its dimerization.

Although apoptosis induced by the CIDE proteins has been characterized by DNA fragmentation and counting of adherent cells undergoing apoptosis (17), the molecular mechanism supporting this biological effect has not been completely elucidated. The requirement of CIDE-B homodimerization and its mitochondrial localization for cell death induction has been recently reported (19). Here, we analyzed the effect of CIDE-B overexpression on the mitochondrial death pathway. We have shown that CIDE-B induces cytochrome *c* release from the mitochondria. Given that cytochrome *c* release from mitochondria during apoptosis is associated with the delivery of caspase-activating molecules (for review, see Ref. 41), we further studied the influence of CIDE-B on caspase activity. We have shown that CIDE-B induces caspase-3 activity. Taken together, our results favor the idea that CIDE-B induces apoptosis through the cytochrome *c*/caspase-9/caspase-3 pathway.

We further demonstrated that NS2 protects cells from the cytochrome *c* release induced by CIDE-B. Indeed, the cytochrome *c* level remaining in the mitochondrial fraction of cells coexpressing NS2 and CIDE-B was higher than that in the mitochondrial fraction of cells expressing CIDE-B alone. Interestingly, experiments performed with HCV transgenic mice expressing the core, E1, E2, and NS2 proteins in the liver showed that Fas-mediated apoptosis is blocked at the mitochondrial level as illustrated by the inhibition of cytochrome *c* release (31). We therefore favor the idea that NS2 may contribute to this previously observed anti-apoptotic effect.

Until now, CIDE-B-induced apoptosis has been exclusively demonstrated *ex vivo* by overexpression of the protein in different established cell lines (17, 19). In this study, we have shown, *in vivo*, that the amount of CIDE-B in normal mice was lowered (3-fold) after viral infection. This result is consistent with the idea that the suppression of pro-apoptotic CIDE-B may cause a defective apoptotic system and thus may be a general mechanism of viral evasion from the host cell defense. It is noteworthy that the effect of viral infection on the reduction of CIDE-B levels was potentiated (35-fold) in transgenic mice expressing HCV proteins. This result is in accordance with the idea that NS2 may be involved in the dramatic CIDE-B protein inhibition, although we cannot exclude that other viral proteins might also be involved in this phenomenon.

Altogether, these observations raise the question of the molecular mechanism by which NS2, a transmembrane protein anchored to the endoplasmic reticulum (33), may bind to and inhibit the death activity of a cytosolic CIDE-B protein, which translocates to mitochondria to fulfill its killing activity. Given that the exact transmembrane topology of NS2 is still not elucidated (33, 37, 44, 45), we suggest that the NS2 C-terminal region harboring the identified CIDE-B-binding site has to be directed to the cytosol. Whether NS2 may trap CIDE-B in the endoplasmic reticulum via binding to its C-terminal domain and thus hindering its mitochondrial localization required for its apoptotic activity or whether NS2 can interfere with CIDE-B dimerization at the mitochondrial site remains to be determined. The latter hypothesis implies that at least some NS2 proteins may also have a cytosolic localization. Further investigations are needed to confirm these hypotheses.

Several interactions between different HCV proteins and cellular partners implicated in apoptosis has already been documented, *e.g.* the core protein and the complement receptor gC1qR (46), the core protein and members of the tumor necrosis factor receptor family (47, 48), E2 and PKR (24, 49), and NS5A and PKR (22, 23). Whereas all these interactions concern nonspecific hepatic proteins involved in apoptotic mechanisms, our study describes the relation between the NS2 protein of a hepatotropic virus and a liver-specific cellular protein, CIDE-B.

We therefore propose that this interaction between NS2 and CIDE-B may be one mechanism that contributes to the viral persistence observed in HCV pathogenesis.

Acknowledgments—We thank Roselyne Primault for confocal microscopy analysis and Virginie Vallet-Erdtmann for critical reading of the manuscript. We thank P. Legrain, G. Inchauspé, F. Russo-Marie, G. Nunez, and X. Wang for the kind gifts of reagents.

REFERENCES

1. O'Brien, V. (1998) *J. Gen. Virol.* **79,** 1833–1845
2. Everett, H., and McFadden, G. (1999) *Trends Microbiol.* **7,** 160–165
3. Balachandran, S., Kim, C. N., Yeh, W. C., Mak, T. W., Bhalla, K., and Barber, G. N. (1998) *EMBO J.* **17,** 6888–6902
4. Balachandran, S., Roberts, P. C., Kipperman, T., Bhalla, K. N., Compans, R. W., Archer, D. R., and Barber, G. N. (2000) *J. Virol.* **74,** 1513–1523
5. Gil, J., and Esteban, M. (2000) *Apoptosis* **5,** 107–114
6. Hiramatsu, N., Hayashi, N., Katayama, K., Mochizuki, K., Kawanishi, Y., Kasahara, A., Fusamoto, H., and Kamada, T. (1994) *Hepatology* **19,** 1354–1359
7. Seino, K., Kayagaki, N., Takeda, K., Fukao, K., Okumura, K., and Yagita, H. (1997) *Gastroenterology* **113,** 1315–1322
8. Kondo, T., Suda, T., Fukuyama, H., Adachi, M., and Nagata, S. (1997) *Nat. Med.* **3,** 409–413
9. Nagata, S. (1997) *Cell* **88,** 355–365
10. Li, H., Zhu, H., Xu, C. J., and Yuan, J. (1998) *Cell* **94,** 491–501
11. Salvesen, G. S., and Dixit, V. M. (1999) *Proc. Natl. Acad. Sci. U. S. A.* **96,** 10964–10967
12. Li, P., Nijhawan, D., Budihardjo, I., Srinivasula, S. M., Ahmad, M., Alnemri, E. S., and Wang, X. (1997) *Cell* **91,** 479–489
13. Liu, X., Zou, H., Slaughter, C., and Wang, X. (1997) *Cell* **89,** 175–184
14. Enari, M., Sakahira, H., Yokoyama, H., Okawa, K., Iwamatsu, A., and Nagata, S. (1998) *Nature* **391,** 43–50
15. Sakahira, H., Enari, M., and Nagata, S. (1998) *Nature* **391,** 96–99
16. Sakahira, H., Takemura, Y., and Nagata, S. (2001) *Arch. Biochem. Biophys.* **388,** 91–99
17. Inohara, N., Koseki, T., Chen, S., Wu, X., and Nunez, G. (1998) *EMBO J.* **17,** 2526–2533
18. Lugovskoy, A. A., Zhou, P., Chou, J. J., McCarty, J. S., Li, P., and Wagner, G. (1999) *Cell* **99,** 747–755
19. Chen, Z., Guo, K., Toh, S. Y., Zhou, Z., and Li, P. (2000) *J. Biol. Chem.* **275,** 22619–22622
20. Lohmann, V., Korner, F., Koch, J., Herian, U., Theilmann, L., and Bartenschlager, R. (1999) *Science* **285,** 110–113
21. Bukh, J., Pietschmann, T., Lohmann, V., Krieger, N., Faulk, K., Engle, R. E., Govindarajan, S., Shapiro, M., St. Claire, M., and Bartenschlager, R. (2002) *Proc. Natl. Acad. Sci. U. S. A.* **99,** 14416–14421
22. Gale, M. J., Jr., Korth, M. J., Tang, N. M., Tan, S. L., Hopkins, D. A., Dever, T. E., Polyak, S. J., Gretch, D. R., and Katze, M. G. (1997) *Virology* **230,** 217–227
23. Gale, M., Jr., Blakely, C. M., Kwieciszewski, B., Tan, S. L., Dossett, M., Tang, N. M., Korth, M. J., Polyak, S. J., Gretch, D. R., and Katze, M. G. (1998) *Mol. Cell. Biol.* **18,** 5208–5218
24. Taylor, D. R., Shi, S. T., Romano, P. R., Barber, G. N., and Lai, M. M. (1999) *Science* **285,** 107–110
25. Levin, D., and London, I. M. (1978) *Proc. Natl. Acad. Sci. U. S. A.* **75,** 1121–1125
26. Ruggieri, A., Harada, T., Matsuura, Y., and Miyamura, T. (1997) *Virology* **229,** 68–76
27. Dumoulin, F. L., van dem Bussche, A., Sohne, J., Sauerbruch, T., and Spengler, U. (1999) *Eur. J. Clin. Invest.* **29,** 940–946
28. Honda, A., Arai, Y., Hirota, N., Sato, T., Ikegaki, J., Koizumi, T., Hatano, M., Kohara, M., Moriyama, T., Imawari, M., Shimotohno, K., and Tokuhisa, T. (1999) *J. Med. Virol.* **59,** 281–289
29. Hahn, C. S., Cho, Y. G., Kang, B. S., Lester, I. M., and Hahn, Y. S. (2000) *Virology* **276,** 127–137
30. Honda, A., Hatano, M., Kohara, M., Arai, Y., Hartatik, T., Moriyama, T., Imawari, M., Koike, K., Yokosuka, O., Shimotohno, K., and Tokuhisa, T. (2000) *J. Hepatol.* **33,** 440–447
31. Machida, K., Tsukiyama-Kohara, K., Seike, E., Tone, S., Shibasaki, F., Shimizu, M., Takahashi, H., Hayashi, Y., Funata, N., Taya, C., Yonekawa, H., and Kohara, M. (2001) *J. Biol. Chem.* **276,** 12140–12146
32. Kalkeri, G., Khalap, N., Garry, R. F., Fermin, C. D., and Dash, S. (2001) *Virology* **282,** 26–37
33. Santolini, E., Pacini, L., Fipaldini, C., Migliaccio, G., and Monica, N. (1995) *J. Virol.* **69,** 7461–7471
34. Lohmann, V., Koch, J. O., and Bartenschlager, R. (1996) *J. Hepatol.* **24,** 11–19
35. Kolykhalov, A. A., Mihalik, K., Feinstone, S. M., and Rice, C. M. (2000) *J. Virol.* **74,** 2046–2051
36. Pieroni, L., Santolini, E., Fipaldini, C., Pacini, L., Migliaccio, G., and La Monica, N. (1997) *J. Virol.* **71,** 6373–6380
37. Pallaoro, M., Lahm, A., Biasiol, G., Brunetti, M., Nardella, C., Orsatti, L., Bonelli, F., Orru, S., Narjes, F., and Steinkuhler, C. (2001) *J. Virol.* **75,** 9939–9946
38. Flajolet, M., Rotondo, G., Daviet, L., Bergametti, F., Inchauspe, G., Tiollais, P., Transy, C., and Legrain, P. (2000) *Gene* (*Amst.*) **242,** 369–379
39. Cadwell, R. C., and Joyce, G. F. (1992) *PCR Methods Applications* **2,** 28–33
40. Kim, J. E., Song, W. K., Chung, K. M., Back, S. H., and Jang, S. K. (1999) *Arch. Virol.* **144,** 329–343
41. Wang, X. (2001) *Genes Dev.* **15,** 2922–2933
42. Lerat, H., Honda, M., Beard, M. R., Loesch, K., Sun, J., Yang, Y., Okuda, M., Gosert, R., Xiao, S. Y., Weinman, S. A., and Lemon, S. M. (2002) *Gastroenterology* **122,** 352–365
43. Grakoui, A., Hanson, H. L., and Rice, C. M. (2001) *Hepatology* **33,** 489–495
44. Mak, P., Palant, O., Labonte, P., and Plotch, S. (2001) *FEBS Lett.* **503,** 13–18
45. Yamaga, A. K., and Ou, J. H. (2002) *J. Biol. Chem.* **277,** 33228–33234
46. Kittlesen, D. J., Chianese-Bullock, K. A., Yao, Z. Q., Braciale, T. J., and Hahn, Y. S. (2000) *J. Clin. Invest.* **106,** 1239–1249
47. Matsumoto, M., Hsieh, T. Y., Zhu, N., VanArsdale, T., Hwang, S. B., Jeng, K. S., Gorbalenya, A. E., Lo, S. Y., Ou, J. H., Ware, C. F., and Lai, M. M. (1997) *J. Virol.* **71,** 1301–1309
48. Zhu, N., Khoshnan, A., Schneider, R., Matsumoto, M., Dennert, G., Ware, C., and Lai, M. M. (1998) *J. Virol.* **72,** 3691–3697
49. Pavio, N., Taylor, D. R., and Lai, M. M. (2002) *J. Virol.* **76,** 1265–1272
50. Fromont-Racine, M., Rain, J. C., and Legrain, P. (1997) *Nat. Genet.* **16,** 277–282
51. Inchauspé, G., Zebedee, S., Lee, D. H., Sugitani, M., Nasoff, M., and Prince, A. M. (1991) *Proc. Natl. Acad. Sci. U. S. A.* **88,** 10292–10296
52. Erdtmann, L., Janvier, K., Raposo, G., Craig, H. M., Benaroch, P., Berlioz-Torrent, C., Guatelli, J. C., Benarous, R., and Benichou, S. (2000) *Traffic* **1,** 871–883
53. Liu, L. X., Margottin, F., Le Gall, S., Schwartz, O., Selig, L., Benarous, R., and Benichou, S. (1997) *J. Biol. Chem.* **272,** 13779–13785
54. Frangioni, J. V., and Neel, B. G. (1993) *Anal. Biochem.* **210,** 179–187
55. Le Gall, S., Erdtmann, L., Benichou, S., Berlioz-Torrent, C., Liu, L., Benarous, R., Heard, J. M., and Schwartz, O. (1998) *Immunity* **8,** 483–495
56. Stennicke, H. R., and Salvesen, G. S. (1997) *J. Biol. Chem.* **272,** 25719–25723
57. Klonjkowski, B., Gilardi-Hebenstreit, P., Hadchouel, J., Randrianarison, V., Boutin, S., Yeh, P., Perricaudet, M., and Kremer, E. J. (1997) *Hum. Gene Ther.* **8,** 2103–2115